Lysosomal cystine efflux opposes mTORC1 reactivation through the TCA cycle

Patrick Jouandin[1†*], Zvonimir Marelja[2†], Andrey A Parkhitko[1], Miriam Dambowsky[2], John M Asara[3,4], Ivan Nemazanyy[5], Matias Simons[2§*] and Norbert Perrimon[1,6§*]

[1] Department of Genetics, Harvard Medical School, Boston, MA, 02115, USA

[2] Laboratory of Epithelial Biology and Disease, *Imagine* Institute, Université Paris-Descartes-Sorbonne Paris Cité, 75015 Paris, France

[3] Division of Signal Transduction, Beth Israel Deaconess Medical Center, Boston, MA 02115, USA

[4] Department of Medicine, Harvard Medical School, Boston, MA 02175, USA

[5] Platform for Metabolic Analyses, Institut Necker Enfants Malades, 75014, Paris, France

[6] Howard Hughes Medical Institute, Harvard Medical School, Boston, MA, 02115, USA

[†] These authors contributed equally to this work

[§] These authors contributed equally to this work

[*]Corresponding authors:

Patrick Jouandin: Patrick_Jouandin@hms.harvard.edu

Matias Simons: matias.simons@institutimagine.org

Norbert Perrimon: perrimon@receptor.med.harvard.edu

Tel: (617) 432-7673 | Fax: (617) 432-7688

ABSTRACT

The highly regulated process of adapting to cellular nutritional status depends on lysosomal mTORC1 (mechanistic Target of Rapamycin Complex 1), that integrates nutrients availability via the sensing of amino acids to promote growth and anabolism[1]. Nutrient restriction inhibits mTORC1 activity, which in turn induces autophagy, a crucial adaptive process that recycles internal nutrient stores to promote survival[2]. However, as successful amino acid recycling through autophagic degradation reactivates mTORC1 signaling over time[3,4], it is unclear how autophagy can be maintained during prolonged starvation. Here, we show that one particular amino acid, cysteine, acts in a feedback loop to limit mTORC1 reactivation *in vivo*. We provide evidence that lysosomal export of cystine through the cystine transporter cystinosin fuels a metabolic pathway that suppresses mTORC1 signaling and maintains autophagy during starvation. This pathway involves reduction to cysteine, cysteine catabolism to acetyl-CoA and subsequent fueling of the TCA cycle. Accordingly, the starvation sensitivity phenotype of animals lacking cystinosin is rescued by dietary supplementation with cysteine and TCA cycle components as well as by reducing mTORC1 activity. We propose that cysteine mediates a communication between lysosomes and mitochondria to control mTORC1 signaling under prolonged starvation, highlighting how changes in nutrient availability divert the fate of an amino acid into a growth suppressive program to maintain the balance between nutrient supply and consumption.

Organisms constantly cope with variations in nutrient supply by adjusting metabolism, a process controlled by the major growth regulator mTORC1. Nutrient scarcity inhibits mTORC1 to limit growth and promote catabolic programs, including autophagy. Autophagy involves the sequestration of cytosolic material into autophagosomes that fuse with lysosomes for cargo degradation and recycling. Efficient lysosomal degradation generates new amino acids that in turn reactivate mTORC1[3-6]. However, how mTORC1 inhibition and activation is balanced over the course of starvation remains unclear.

To study this process *in vivo,* we used the *Drosophila* larval fat body, an organ analogous to the liver and adipose tissue in mammals with important functions during starvation[2,7]. As in mammalian cells, prolonged starvation led to mTORC1 reactivation in fat bodies, which was dependent on autophagy induction (Fig. 1a, b and Extended Data Fig 1a). To identify signals controlling mTORC1 activity upon fasting, we focused on amino acids and performed an unbiased approach to analyze growth of fasted larvae under single amino acid supplementation (Supplementary Methods). Unexpectedly, this screen revealed cysteine as a unique amino acid associated with growth suppressive properties (Supplementary Text 1, Fig. 1c and Extended Data Fig. 1b-e). This process required mTORC1 inhibition as constitutive activation of mTORC1 in Gator1 mutants (*nprl2*$^{-/-}$)[8] partially restored growth under cysteine supplementation (Fig. 1d). Consistently, cysteine treatment partially inhibited mTORC1 activity in fat bodies (Extended Data Fig. 1f).

We reasoned that, as lysosomal efflux of nutrients promotes mTORC1 reactivation[3], cysteine could limit this process. In physiological conditions, cellular cysteine can either be synthesized in the cytosol or transported as cystine from the extracellular space by the Xc^- antiporter[9] and by cystinosin from the lysosome[10] (Fig. 1e). Thus, we analyzed whether cysteine recycling through cystinosin opposes mTORC1 reactivation upon fasting. Cystinosin is encoded by *CTNS*, a gene mutated in the lysosomal storage disorder cystinosis[11]. The *Drosophila* genome contains a single ortholog of *CTNS* (*CG17119*), hereafter referred to as *dCTNS*. Endogenous tagging of cystinosin in *Drosophila* confirmed its specific lysosomal localization in fat body cells, and *dCTNS*$^{-/-}$ larvae showed accumulation of cystine (Extended Data Fig. 2a-c), consistent with a role for cystinosin in lysosomal cystine transport. In fed conditions, control and *dCTNS*$^{-/-}$ larvae showed similar cysteine levels, likely reflecting dietary intake as the main source of cysteine (Fig.1f). However, upon fasting, cysteine levels dropped in *dCTNS* $^{-/-}$ larvae, and maintenance of cysteine levels required autophagy (Fig. 1f, g). Thus, we conclude that cystinosin recycles cysteine from autophagic degradation upon fasting.

Next, we analyzed the role of cystinosin on mTORC1 reactivation during fasting. *dCTNS* knockdown in larval fat body (*lpp-gal4*) did not affect mTORC1 during the early phase of starvation. However, it slightly increased mTORC1 reactivation upon prolonged starvation (Fig. 1h). Analysis of *dCTNS*$^{-/-}$ fat body clones showed that this effect was cell autonomous (Extended Data Fig. 2d) and sufficient to compromise maintenance of autophagy (Extended Data Fig. 2e). Conversely, *dCTNS* overexpression increased cysteine levels (Fig. 1i), which caused downregulation of mTORC1 and induction of autophagy (Fig. 1i and Extended Data Fig. 2e). Similar to cysteine treatment, *dCTNS* overexpression caused a developmental delay in both fed and starved conditions (Extended data Fig. 2f), in agreement with mTORC1 activity promoting growth during development. Finally, *dCTNS* loss of function led to starvation sensitivity in both larvae and adult animals (leading to a developmental delay in larvae, see Supplementary text 2), consistent with the importance of mTORC1 downregulation and autophagy induction for survival upon fasting[2] (Extended Data Fig. 2g-i). This was dependent on cystine efflux as treatment with cysteamine (which exports cystine out of the lysosome independently of cystinosin[12]) rescued the starvation sensitivity of *dCTNS*$^{-/-}$ animals (Extended Data Fig. 2k). In addition, treatment with low concentration of cysteine (that did not affect development of control animals) and the mTORC1 inhibitor rapamycin, respectively, also restored resistance to starvation of *dCTNS*$^{-/-}$ animals (Fig. 1j-l), indicating that cystinosin controls mTORC1 through cytosolic cysteine. Altogether, we demonstrate that lysosomal-derived cysteine restricts mTORC1 reactivation to a threshold that maintains autophagy upon prolonged fasting.

Following reduction of cytosolic cystine to cysteine[13], cysteine catabolism generates byproducts[14,15]. To discriminate between the effect of cysteine and these byproducts on mTORC1 inhibition, we sought to genetically suppress cysteine degradation. In mammals, cysteine degradation in liver and adipose tissues is catalyzed by cysteine dioxygenase type 1 (CDO1), a nucleo-cytoplasmic enzyme that generates cysteine sulfinate (CSA), a precursor for pyruvate and taurine synthesis[14,16,17] (Fig. 2a). The *Drosophila* genome contains a single ortholog of *CDO1* encoded by *CG5493* (referred to as *dCDO*) that is strongly expressed in

the fat body (Extended Data Fig. 3a). *dCDO*$^{-/-}$ larvae showed decreased levels of CSA and taurine, and *dCDO* knockdown in the fat body led to cysteine accumulation, particularly in larvae fed cysteine-enriched food, consistent with a role for *d*CDO in cysteine degradation (Fig. 2b; Extended Data Fig. 3b). Further, inhibition of mTORC1 by cysteine supplementation was suppressed in *dCDO*$^{-/-}$ animals (Fig. 2c), suggesting that cysteine requires degradation to CSA to control mTORC1. Accordingly, CSA supplementation had a similar effect than cysteine on growth and mTORC1 activity (Extended Data Fig. 3c, d). In addition, downregulation of *dCDO* in the larval fat body suppressed the developmental delay and the inhibition of mTORC1 induced by *dCTNS* overexpression, whereas CSA treatment restored the inhibition of mTORC1 (Extended Data Fig. 2d, e; Extended Data Fig. 3e). Consistently, *dCDO* knockdown in the fat body led to a stronger reactivation of mTORC1 under prolonged fasting (Fig. 2f; Extended Data Fig. 3f, g). Finally, aberrant mTORC1 reactivation following *dCDO* knockdown impaired fasting-induced autophagy (Fig. 2g). In sum, our data show that lysosomal cystine efflux and subsequent cysteine degradation into CSA opposes mTORC1 reactivation to maintain autophagy upon prolonged fasting.

Since amino acids and amino acid catabolism are potent activators of mTORC1[18,19], our finding that cysteine degradation limits mTORC1 reactivation is unexpected and prompted further analysis of the respective downstream events. As CSA is used for the synthesis of pyruvate and taurine, we first tested their effects on growth. Treatment with pyruvate but not with taurine, resembled the effects of cysteine and CSA on growth (Extended Data Fig. 4a), hinting at a role for the cysteine/pyruvate metabolic route in the control of mTORC1 reactivation. Consistently, supplementing food with pyruvate partially rescued starvation sensitivity of *dCTNS*$^{-/-}$ animals (Fig. 3a). In accordance with pyruvate function in fueling the TCA cycle, animals treated with excess cysteine showed increased levels of pyruvate and TCA cycle intermediates, particularly upon starvation (Fig. 3b, c). Accordingly, in physiological conditions (without cysteine supplementation), the level of many TCA cycle intermediates measured either from whole larvae or the fat body acutely increased during starvation, eventually reaching a steady state comparable to the levels of fed animals (Extended Data Fig. 4b-d). Essential amino acids were acutely depleted upon fasting, whereas the level of non-essential amino acids that requires TCA cycle activity was maintained. Importantly, maintenance of the level of TCA cycle intermediates required cysteine, as *dCTNS*$^{-/-}$ animals showed a pronounced depletion of pyruvate and TCA cycle intermediates upon prolonged fasting but not in fed conditions (Fig. 3d). By contrast, overexpression of *dCTNS* in fed animals led to opposite results (Fig. 3d). In sum, these data indicate that cysteine catabolism maintains TCA cycle activity upon fasting.

Pyruvate can contribute carbons to the TCA cycle through two metabolic routes. One serves an anaplerotic function to replenish oxaloacetate through the enzyme pyruvate carboxylase (PC), while the other contributes carbon in the form of acetyl-CoA through the pyruvate dehydrogenase complex (PDHc) (Fig. 3b). [U-$^{13}C_3$]cysteine labeling experiments *in vivo* revealed incorporation of cysteine carbons into CSA and acetyl-CoA in a *dCDO*-dependent manner in dissected fat bodies, indicating that cysteine/CSA provides substrate for PDHc (Extended Data Fig. 4e). However, due to very low labeling in the TCA cycle (see details in Supplementary text 3, Extended Data Fig. 5), we could not rule out a role for minimal cysteine anaplerosis through PC. Thus, we further used genetics to discriminate between PC and PDHc pathways on the regulation of mTORC1 by cysteine. Knockdown of *PC* (*pcb*/*CG1516*) suppressed mTORC1 reactivation upon fasting, whereas knockdown of pyruvate dehydrogenase phosphatase (*pdp*), which leads to PDHc inhibition[20], caused a stronger reactivation of mTORC1 (Fig. 4a, b). This was supported by silencing *pdha* (the rate limiting enzyme of PDHc) in both entire fat bodies and in clones (Fig. 4c, Extended data Fig. 6a). Accordingly, inhibition of mTORC1 by *dCTNS* overexpression or cysteine supplementation was suppressed by knockdown of *pdp* (Fig. 4d, Extended data Fig. 6b). Finally, inhibition of PDHc impaired autophagy in larvae and triggered starvation intolerance in adult animals, similar to inhibition of *dCTNS* and *dCDO* (Fig. 4e, Extended data Fig. 6c). Thus, lysosomal cystine efflux and subsequent degradation to pyruvate opposes mTORC1 signaling reactivation through PDHc-dependent entry of acetyl-CoA into the TCA cycle.

To analyze whether the levels of particular TCA cycle intermediates downstream acetyl-CoA was relevant in the regulation of mTORC1, we screened for their effect on growth. We focused on fumarate, because it was the only TCA cycle intermediate associated with growth retardation (Extended data Fig. 6d, e). Fumarate treatment suppressed mTORC1 activity and rescued the effect of *dCDO* knockdown on mTORC1 in a *dCTNS* overexpression background (Extended data Fig. 6f, Fig. 4f). Finally, fumarate treatment partially rescued starvation sensitivity of *dCTNS*$^{-/-}$ animals (Fig. 4g), suggesting that the level of TCA cycle intermediates act

downstream cystinosin during inhibition of mTORC1 activity. Alternatively, or in parallel, acetyl-CoA from cysteine could directly increase fumarate production through stabilization of cofactors required maximal activity of the fumarate-producing succinate dehydrogenase complex (complex II), as recently described[21]. In sum, we demonstrate that upon prolonged starvation, cysteine degradation to acetyl-CoA limits mTORC1 signaling reactivation through the TCA cycle to maintain autophagy (Fig. 4h).

Maintaining cellular homeostasis upon nutrient shortage is an important challenge for all animals. On the one hand, downregulation of mTORC1 is necessary to limit translation, reduce growth rates and engage autophagy. On the other hand, minimal mTORC1 activity is required to promote lysosomes biogenesis, thus maintaining autophagic degradation necessary for survival[22]. Here, we identify another critical layer of regulation that prevents reactivation of mTORC1 above a threshold that would compromise autophagy and survival upon fasting. Thus, reactivation of mTORC1 upon fasting is not passively controlled by the extent of nutrient remobilization, but instead is actively regulated by a mitochondrial pathway that maintains autophagy during starvation. Interestingly, this pathway is initiated by autophagy itself, as autophagic protein degradation controls cystine availability that further limits mTORC1 signaling through the TCA cycle.

Whether particular TCA cycle metabolites such as fumarate directly mediate mTORC1 inhibition remains unclear. Alternatively, acetyl-CoA from cysteine could promote incorporation of anaplerotic inputs into the TCA cycle at the expense of their use for biosynthesis of mTORC1-activating metabolites. Another open question concerns the crosstalk with mTORC1-activating pathways involving the TCA cycle. Our data show, for example, that knockdown of PC that replenishes oxaloacetate suppresses mTORC1 reactivation during fasting, whereas mitochondrial acetyl-CoA metabolism derived from cysteine via PDHc limits mTORC1 reactivation to a certain threshold. By contrast, cytosolic acetyl-CoA derived from leucine metabolism has recently been described to promote S6K phosphorylation through acetylation of mTORC1 regulators[23]. This illustrates how the source and fate of acetyl-CoA dictates its differential roles for mTORC1 activity. Further studies will therefore be required to understand exactly how different inputs in the TCA cycle interact to adjust mTORC1 activity, and how cysteine catabolism affects this system.

REFERENCES

1 Wolfson, R. L. & Sabatini, D. M. The Dawn of the Age of Amino Acid Sensors for the mTORC1 Pathway. *Cell Metab* **26**, 301-309, doi:10.1016/j.cmet.2017.07.001 (2017).

2 Scott, R. C., Schuldiner, O. & Neufeld, T. P. Role and regulation of starvation-induced autophagy in the Drosophila fat body. *Dev. Cell* **7**, 167-178, doi:10.1016/j.devcel.2004.07.009 (2004).

3 Tan, H. W. S., Sim, A. Y. L. & Long, Y. C. Glutamine metabolism regulates autophagy-dependent mTORC1 reactivation during amino acid starvation. *Nature Communications* **8**, 338, doi:10.1038/s41467-017-00369-y (2017).

4 Yu, L. *et al.* Termination of autophagy and reformation of lysosomes regulated by mTOR. *Nature* **465**, 942-946, doi:10.1038/nature09076 (2010).

5 Lin, T.-C. *et al.* Autophagy: Resetting glutamine-dependent metabolism and oxygen consumption. *Autophagy* **8**, 1477-1493, doi:10.4161/auto.21228 (2012).

6 Wyant, G. A. *et al.* NUFIP1 is a ribosome receptor for starvation-induced ribophagy. *Science* **360**, 751-758, doi:10.1126/science.aar2663 (2018).

7 Colombani, J. *et al.* A nutrient sensor mechanism controls Drosophila growth. *Cell* **114**, 739-749 (2003).

8 Wei, Y. & Lilly, M. A. The TORC1 inhibitors Nprl2 and Nprl3 mediate an adaptive response to amino-acid starvation in Drosophila. *Cell Death Differ.* **21**, 1460-1468, doi:10.1038/cdd.2014.63 (2014).

9 Conrad, M. & Sato, H. The oxidative stress-inducible cystine/glutamate antiporter, system x (c) (-) : cystine supplier and beyond. *Amino Acids* **42**, 231-246, doi:10.1007/s00726-011-0867-5 (2012).

10 Cherqui, S. & Courtoy, P. J. The renal Fanconi syndrome in cystinosis: pathogenic insights and therapeutic perspectives. *Nat Rev Nephrol* **13**, 115-131, doi:10.1038/nrneph.2016.182 (2017).

11 Town, M. *et al.* A novel gene encoding an integral membrane protein is mutated in nephropathic cystinosis. *Nat. Genet.* **18**, 319-324, doi:10.1038/ng0498-319 (1998).

12 Gahl, W. A., Tietze, F., Butler, J. D. & Schulman, J. D. Cysteamine depletes cystinotic leucocyte granular fractions of cystine by the mechanism of disulphide interchange. *Biochem. J.* **228**, 545-550 (1985).

13 Pader, I. *et al.* Thioredoxin-related protein of 14 kDa is an efficient L-cystine reductase and S-denitrosylase. *Proc Natl Acad Sci U S A* **111**, 6964-6969, doi:10.1073/pnas.1317320111 (2014).

14 Griffith, O. W. Cysteinesulfinate metabolism. altered partitioning between transamination and decarboxylation following administration of beta-methyleneaspartate. *J. Biol. Chem.* **258**, 1591-1598 (1983).

15 Singer, T. P. & Kearney, E. B. Intermediary metabolism of L-cysteinesulfinic acid in animal tissues. *Arch Biochem Biophys* **61**, 397-409, doi:https://doi.org/10.1016/0003-9861(56)90363-0 (1956).

16 Ueki, I. *et al.* Knockout of the murine cysteine dioxygenase gene results in severe impairment in ability to synthesize taurine and an increased catabolism of cysteine to hydrogen sulfide. *Am J Physiol Endocrinol Metab* **301**, E668-684, doi:10.1152/ajpendo.00151.2011 (2011).

17 Parsons, R. B., Ramsden, D. B., Waring, R. H., Barber, P. C. & Williams, A. C. Hepatic localisation of rat cysteine dioxygenase. *J Hepatol* **29**, 595-602, doi:https://doi.org/10.1016/S0168-8278(98)80155-4 (1998).

18 Duran, R. V. *et al.* Glutaminolysis activates Rag-mTORC1 signaling. *Mol. Cell* **47**, 349-358, doi:10.1016/j.molcel.2012.05.043 (2012).

19 Zoncu, R. *et al.* mTORC1 senses lysosomal amino acids through an inside-out mechanism that requires the vacuolar H(+)-ATPase. *Science* **334**, 678-683, doi:10.1126/science.1207056 (2011).

20 Yamamoto, S. *et al.* A drosophila genetic resource of mutants to study mechanisms underlying human genetic diseases. *Cell* **159**, 200-214, doi:10.1016/j.cell.2014.09.002 (2014).

21 Van Vranken, J. G. *et al.* ACP Acylation Is an Acetyl-CoA-Dependent Modification Required for Electron Transport Chain Assembly. *Mol. Cell* **71**, 567-580.e564, doi:10.1016/j.molcel.2018.06.039 (2018).

22 Yu, L. *et al.* Autophagy termination and lysosome reformation regulated by mTOR. *Nature* **465**, 942-946, doi:10.1038/nature09076 (2010).

23 Son, S. M. *et al.* Leucine Signals to mTORC1 via Its Metabolite Acetyl-Coenzyme A. *Cell Metab*, doi:10.1016/j.cmet.2018.08.013 (2018).

24 Mackay, G. M., Zheng, L., van den Broek, N. J. F. & Gottlieb, E. in *Methods Enzymol.* Vol. 561 (ed Christian M. Metallo) 171-196 (Academic Press, 2015).

25 Hahn, K. *et al.* PP2A regulatory subunit PP2A-B' counteracts S6K phosphorylation. *Cell Metab* **11**, 438-444, doi:10.1016/j.cmet.2010.03.015 (2010).

Acknowledgements: We thank Eric Baehrecke, Christen Mirth, Pierre Léopold, Aurelio Teleman, Frederik Wirtz-Peitz, Yohanns Bellaïche, Isabelle Gaugue, Sylvia Sanquer, Anne-Claire Boschat, Mary A. Lilly, the TRIP (http://www.flyrnai.org/TRiP-HOME.html), BDSC and VDRC stock centers for providing stocks and reagents. We thank Corinne Antignac, Lewis C. Cantley, Bruno Gasnier and David M. Sabatini for comments on the manuscript. We thank the Imagine Microscopy platform for assistance with microscopy. This work was funded by the Cystinosis Research Foundation (to P.J., Z.M., M.S. and N.P.), the LAM Foundation Fellowship Award LAM00105E01-15 (to A.P.), National Institutes of Health 5P01CA120964-04 (to J.M.A. and N.P.) and R01AR057352 (to N.P), the ATIP-Avenir program, the Fondation Bettencourt-Schueller (Liliane Bettencourt Chair of Developmental Biology) as well as State funding by the Agence Nationale de la Recherche (ANR) under the “Investissements d’avenir” program (ANR-10-IAHU-01) and the NEPHROFLY (ANR-14-ACHN-0013) grant (to MS.). N.P. is an investigator of the Howard Hughes Medical Institute.

Author Contributions: P.J., Z.M., M.S. and N.P designed the experiments; P.J., Z.M., A.P., M.D., J.A., and I.N performed the experiments; P.J., Z.M., M.S. and N.P. participated in interpretation of data and P.J wrote the manuscript with inputs from Z.M., M.S. and N.P.

FIGURES & LEGENDS

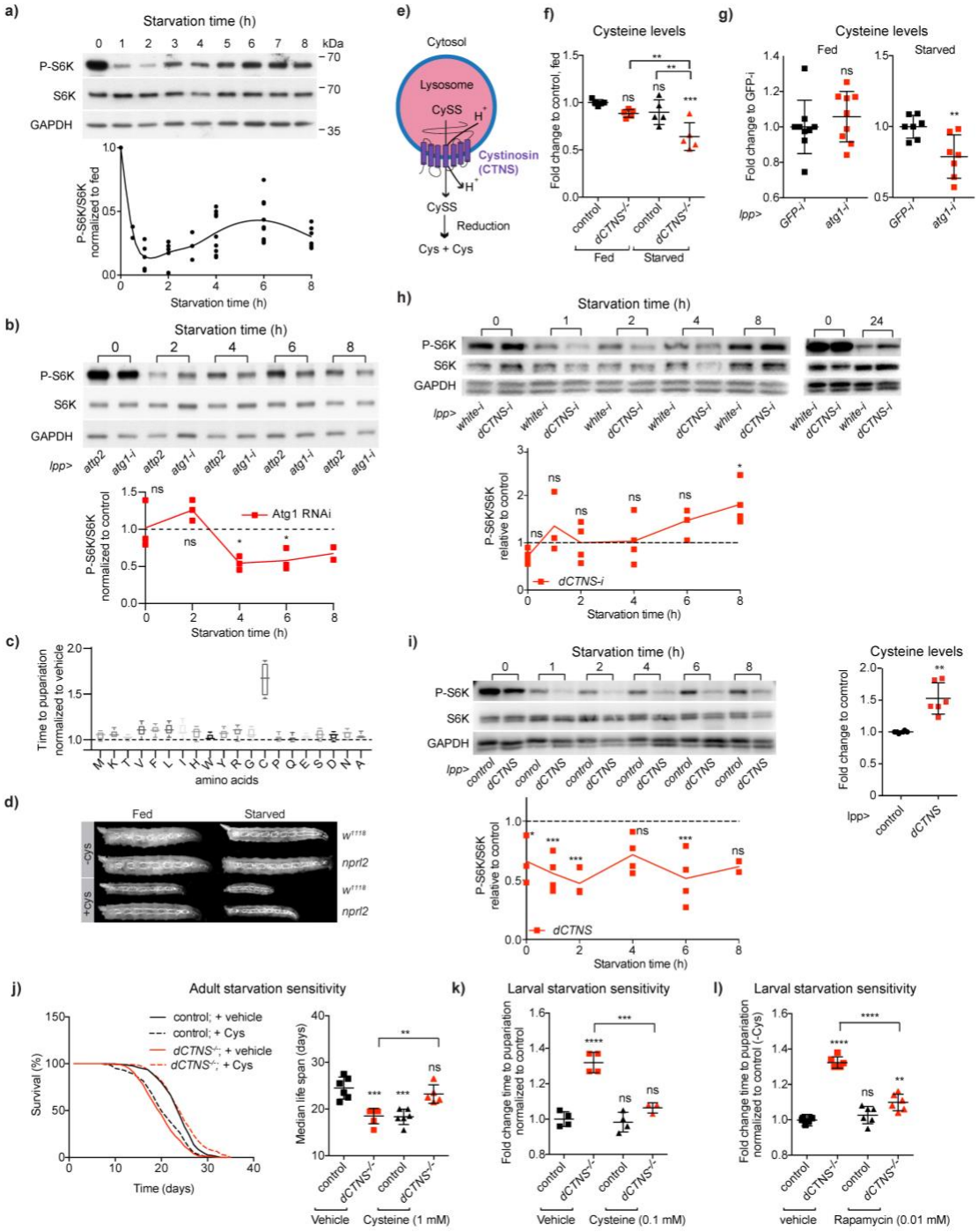

Figure 1: Lysosomal cystine efflux limits mTORC1 reactivation to maintain autophagy upon prolonged fasting. a,b) Prolonged fasting leads to mTORC1 reactivation through autophagy. Phosphorylation levels of the direct mTORC1 target S6K in dissected fat bodies from larvae starved on PBS. c) Amino acid screen reveals cysteine as a growth suppressor. Time to pupariation for larvae fed a minimal diet supplemented with the indicated amino acids *ad libitum*. d) Constitutive mTORC1 activity partially suppresses the effect of cysteine on growth. Fed and fasted, control and Gator1 mutant (*nprl2*) larvae supplemented with 5 mM cysteine or vehicle *ad libitum*. e) Schematic of lysosomal cystine (CySS) efflux through cystinosin. f, g) Cystinosin and autophagy control cysteine levels. Cysteine levels measured from whole fed or starved larvae. Control is GFP RNAi (GFP-i). f) Controls are heterozygote animals (*dCTNS*$^{+/-}$). h) Loss of cystinosin leads to higher mTORC1 reactivation upon prolonged starvation/fasting. P-S6K levels in fat bodies from larvae starved on PBS. i) *dCTNS* overexpression (*lpp>dCTNS*) increases cysteine levels and suppresses mTORC1 activity. Whole body cysteine levels and P-S6K levels in fat body from fed or starved larvae (controls are GFP-i). j-l) Cysteine and rapamycin treatments rescue starvation sensitivity of *dCTNS*$^{-/-}$ animals. Lifespan of adult flies on chemically defined media (j) and developmental time of larvae (k,l). Control is *w*^{1118} (j) and *dCTNS*$^{+/-}$ (k,l).

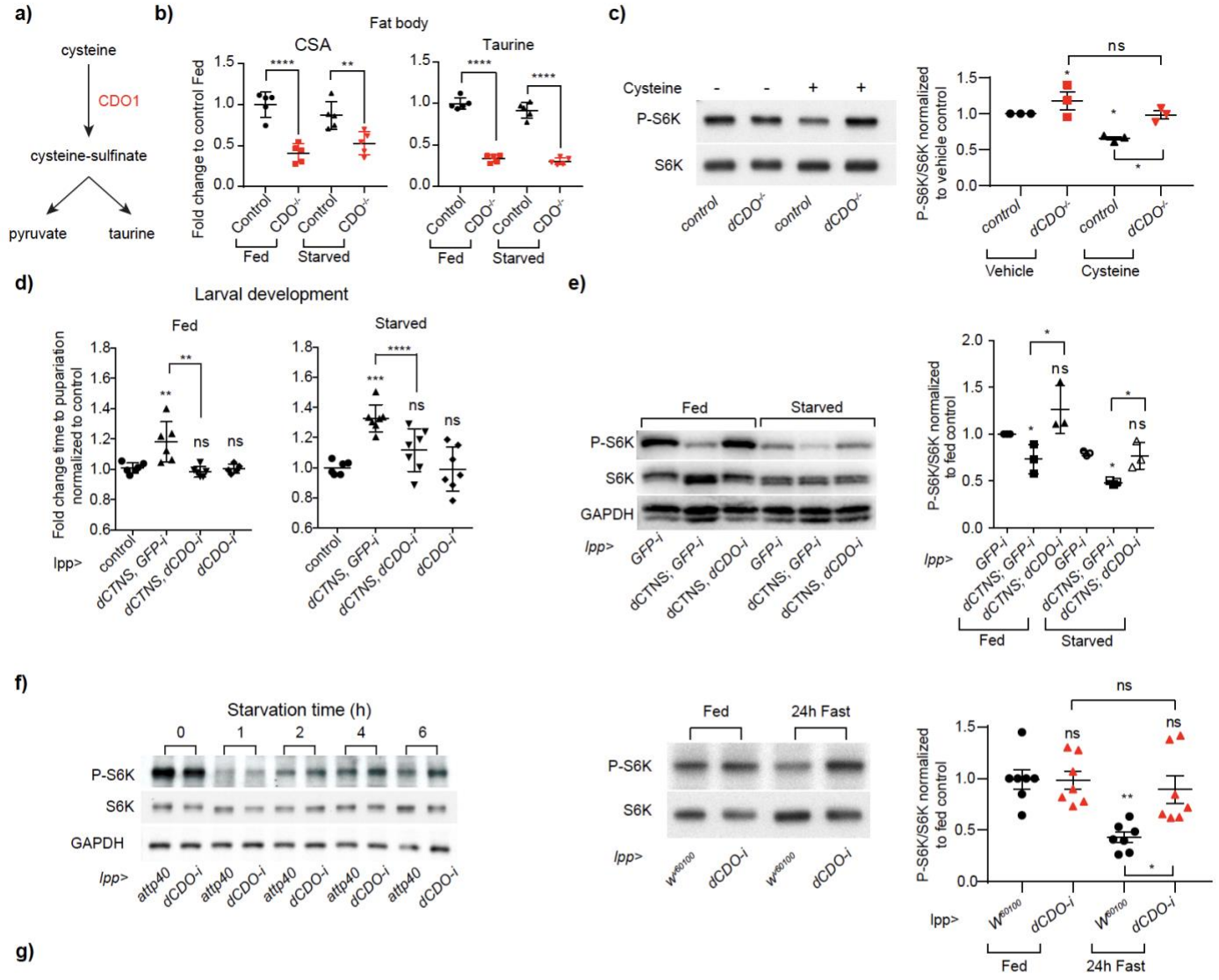

Figure 2: Cysteine requires degradation by dCDO to downregulate mTORC1. a) Schematics of cysteine degradation by CDO1. b) dCDO mediates cysteine degradation. Fold change metabolite abundance measured by LC-MS/MS in larval fat bodies. c) Cysteine suppresses mTORC1 through dCDO. P-S6K levels in fat body from fed larvae supplemented with 1 mM cysteine for 4h. d) Cystinosin suppresses growth through *dCDO*. Developmental timing of larvae. e) Cystinosin inhibits mTORC1 through *dCDO*. P-S6K levels in fat body. Control is GFP-i. f) Loss of *dCDO* leads to higher reactivation of mTORC1 upon prolonged fasting. P-S6K levels in fat body from larvae starved on PBS or fasted. g) dCDO is necessary to maintain autophagy. Flip-out clones (GFP, outlined) in larvae fasted for 6 hours. Scale bar 20 µm.

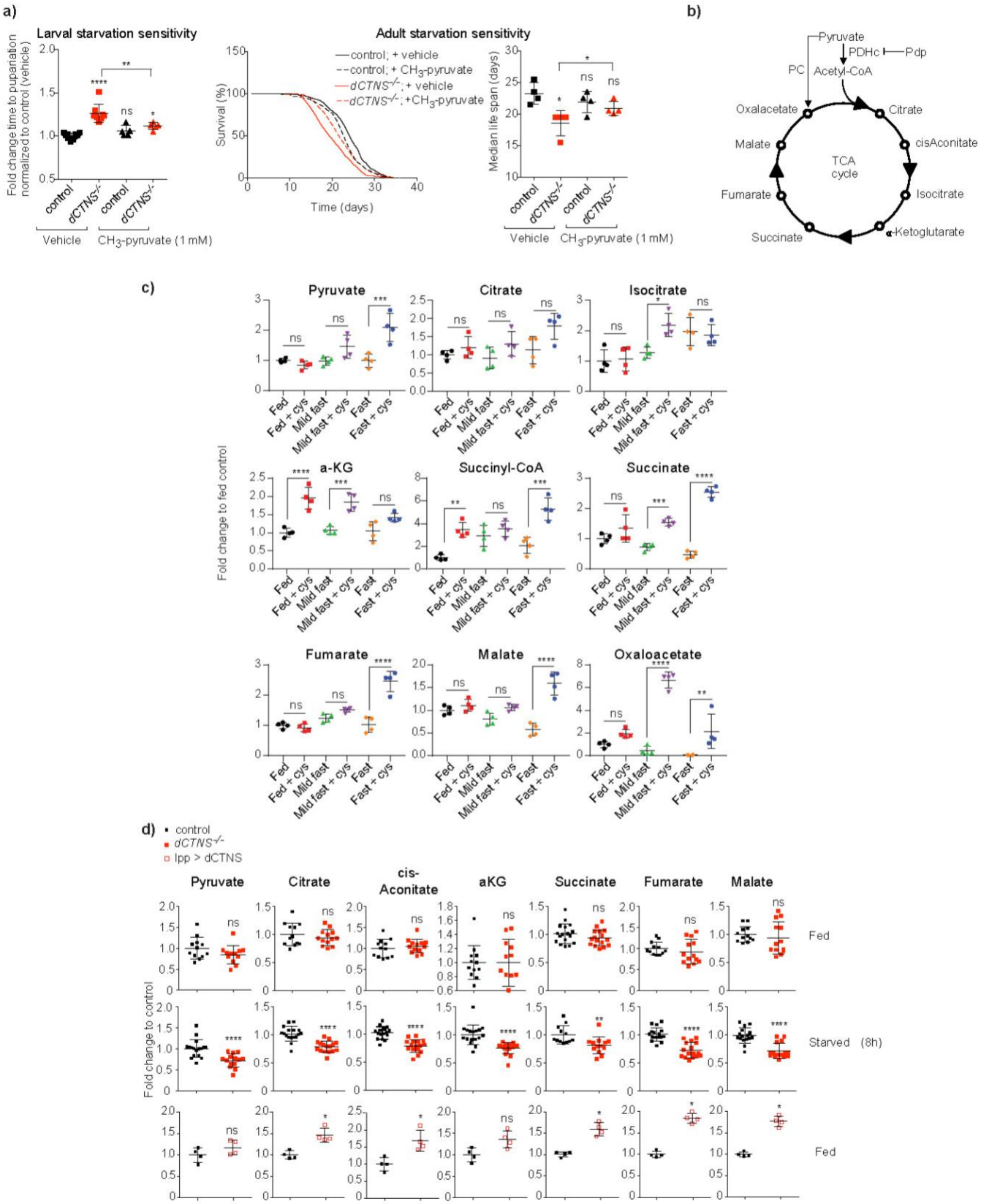

Figure 3: Lysosomal cystine efflux affects the TCA cycle. a) Pyruvate partially restores starvation resistance of *dCTNS*$^{-/-}$ animals. Adult lifespan and larval developmental time. Control is w^{1118}. CH3-pyruvate, methyl-pyruvate. b) Schematic of the TCA cycle. c) Cysteine increases the level of TCA cycle intermediates. Relative metabolites levels measured by LC-MS/MS in whole mid-second instar w^{1118} larvae fed the indicated diet *ad libitum* (fast, fasted; mild fast, mildly fasted), with 10 mM cysteine or vehicle. d) Cystinosin regulates pyruvate and TCA cycle intermediates levels upon starvation. Relative metabolites levels in 80h AEL (after egg laying) larvae fed a full diet *ad libitum* or starved for 10 h on PBS.

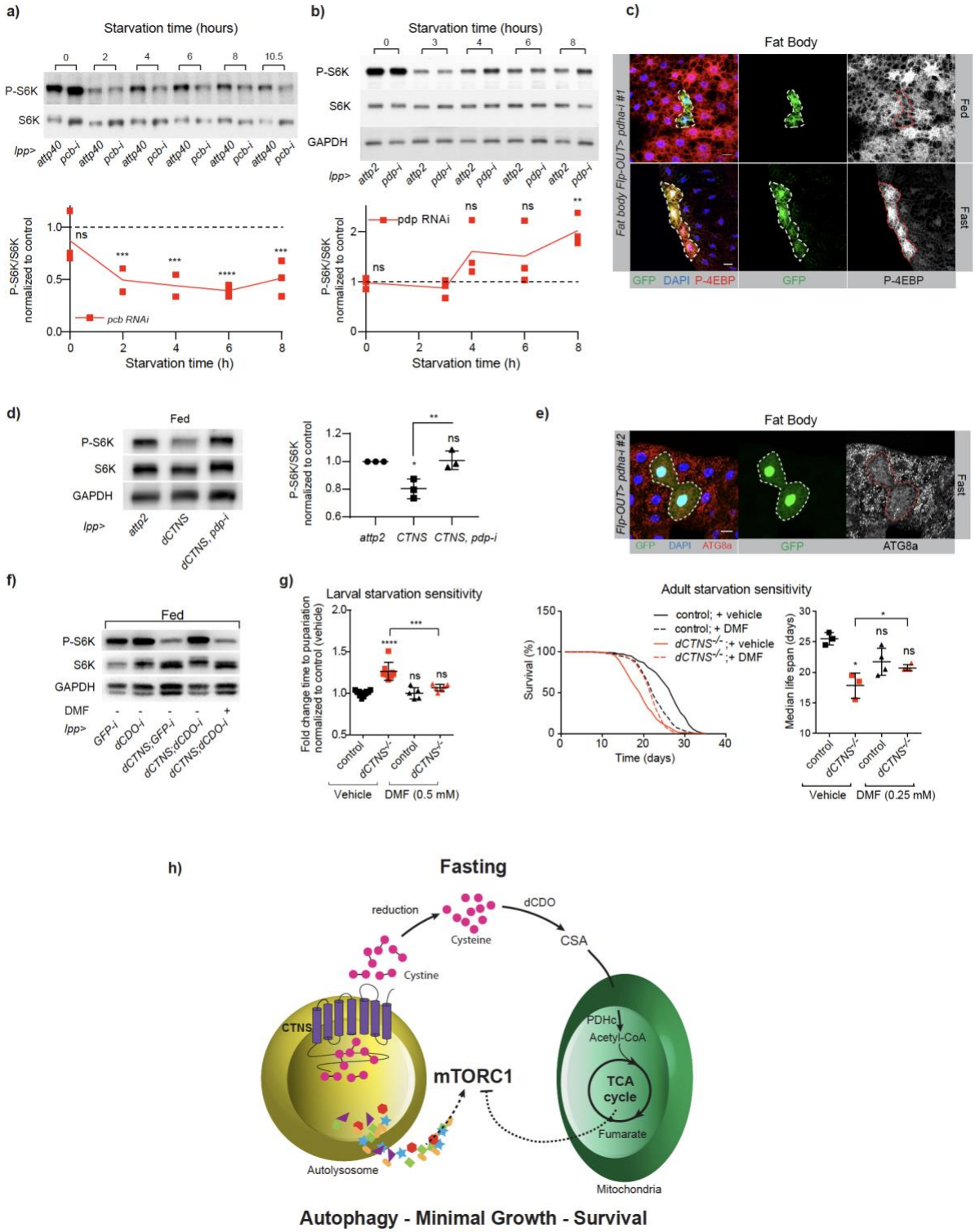

Figure 4: Acetyl-CoA and the TCA cycle mediate the inhibition of mTORC1 by cysteine degradation. a) Knockdown of *pcb* suppresses mTORC1 reactivation upon prolonged fasting. P-S6K levels in fat body from larvae starved on PBS. b) Loss of Pdp leads to higher reactivation of mTORC1 upon prolonged fasting. P-S6K levels in fat body from larvae starved on PBS. c) Loss of Pdha leads to higher reactivation of mTORC1 (evidenced by P-4EBP levels) upon prolonged fasting. Flip-out clones (GFP, outlined) in larvae fed or fasted 12 hours. Scale bar 20 µm. d) Cystinosin suppresses mTORC1 through Pdp. P-S6K levels in fat body from fed larvae. e) Loss of Pdha impairs the induction of autophagy upon starvation. Flip-out clones (GFP, outlined) in fasted larvae. Scale bar 20 µm. f) Fumarate acts downstream cystinosin and dCDO to inhibit mTORC1 signaling. P-S6K levels in fat bodies from larvae treated with vehicle or 5mM dimethyl-fumarate (DMF). g) Fumarate partially restores starvation resistance of *dCTNS*$^{-/-}$ animals. Adult Lifespan and larval developmental time. Control is *w*^{1118}. h) Model: cysteine metabolism maintains autophagy upon prolonged fasting.

Methods

Fly stocks and maintenance

All flies were reared at 25°C and 60% humidity with a 12-h on/off light cycle on lab food. N. Perrimon's lab food: 12.7 g/L deactivated yeast, 7.3 g/L soy flour, 53.5 g/L cornmeal, 0.4 % agar, 4.2 g/L malt, 5.6 % corn syrup, 0.3 % propionic acid, 1% tegosept/ethanol. M. Simon's lab food: 18 g/L deactivated yeast, 10 g/L soy flour, 80 g/L cornmeal, 1% agar, 40 g/L malt, 5% corn syrup, 0.3 % propionic acid, 0.2 % 4-hydroxybenzoic acid methyl ester (nipagin)/ethanol. Density was standardized at least one generation before the experiments. For experiments, larvae were reared on freshly made food. For details on food recipes, drugs and fly stocks used, see Supplementary Methods.

Developmental timing

Three-day-old crosses were used for 3-4 hour periods of egg collection on lab food. Newly hatched L1 larvae were collected 24 hours later for synchronized growth using the indicated diets at a density of 30 animals/vial. The time to develop was monitored by counting the number of animals that underwent pupariation, every two hours in fed conditions or once/twice a day in starved conditions. The time at which half the animals had undergone pupariation is reported, +/-SEM.

Life span experiments

To generate age-synchronized adult flies, larvae were raised on *ad libitum* (means food available at all times with the quantity and frequency of consumption being the free choice of the animal) lab food at low density, transferred to fresh food upon emerging as adults and mated 48h. Animal were anaesthetized with low levels of CO_2 and males sorted at a density of ten per vial. Each condition contained 8-10 vials. Each experiment was repeated at least 3 times and the averages values of each experiment were used for statistical analysis. Flies were transferred to fresh vials three times per week at which point deaths were scored. After ten days, deaths were scored every day.

Metabolite profiling

For whole body metabolic profiling, 25-38 mid-second instar or 8-15 mid-third instar larvae per sample were collected, snap-frozen in liquid nitrogen and stored at -80°C in extraction buffer (4-6 biological replicates/experiment). For fat body metabolic profiling, fat bodies from 35-40 larvae 96h AEL old were dissected in 25 ul PBS, diluted in 300 ul cold extraction buffer and snap frozen. Tissues were homogenized in extraction buffer using 1 mm zirconium beads (Next Advance, ZROB10) in a Bullet Blender tissue homogenizer (Model BBX24, Next Advance). Metabolites were extracted using 80 % (v/v) aqueous methanol (x2 sequential extractions with 300-600 ul) and metabolites pelleted by vacuum centrifugation. Pellets were resuspended in 20 ul HPLC-grade water and metabolomics data were acquired using targeted liquid chromatography tandem mass spectrometry (LC-MS/MS). A 5500 QTRAP hybrid triple quadrupole mass spectrometer (AB/SCIEX) coupled to a Prominence UFLC high-performance LC (HPLC) system (Shimadzu) was used for steady-state analyses of the samples. Selected reaction monitoring (SRM) of 287 polar metabolites using positive/negative switching with hydrophilic interaction LC (HILIC) was performed. Peak areas from the total ion current for each metabolite SRM Q1/Q3 transition were integrated using MultiQuant version 2.1 software (AB/SCIEX). The resulting raw data from the MultiQuant software were normalized by sample weight or protein content measured from equivalent samples and analyzed using Prism informatic software. Alternatively, 75 hours AEL old *dCTNS*$^{+/-}$ (control) or *dCTNS*$^{-/-}$ larvae were transferred either to fresh standard food (fed) or on PBS-soaked (starvation, 8h) Whatman paper. Larvae were rinsed with water, 70% ethanol and PBS to remove food and bacteria. 10-15 mid-third instar larvae per sample were collected, snap-frozen in liquid nitrogen and stored at -80°C until extraction in 50% methanol, 30% ACN, and 20% water. The volume of extraction solution added was adjusted to larvae mass (40mg/ml), samples were vortexed for 5 min at 4°C, and then centrifuged at 16,000 g for 15 minutes at 4°C. Supernatants were collected and analyzed by LC-MS using a QExactive Plus Orbitrap mass spectrometer equipped with an Ion Max source and a HESI II probe and coupled to a Dionex UltiMate 3000 UPLC system (Thermo, USA). An SeQuant ZIC-pHilic column (Millipore) was used for liquid chromatography separation[24]. The aqueous mobile-phase solvent was 20 mM ammonium carbonate plus 0.1% ammonium hydroxide solution and the organic mobile phase was acetonitrile. The metabolites were separated over a linear gradient from 80% organic to 80% aqueous for 15 min and detected across a mass range of 75–1,000 m/z at a resolution of 35,000 (at 200 m/z) with electrospray ionization and polarity switching mode. Lock masses were used to insure mass accuracy below 5 ppm. The

peak areas of different metabolites were determined using TraceFinder software (Thermo) using the exact mass of the singly charged ion and known retention time on the HPLC column. In total, the metabolic profiling experiment was performed three times with 3-7 biological replicates per genotype.

TCA cycle isotopomer method from [U-$^{13}C_3$]cysteine and [U-$^{13}C_6$]glucose

Fed and starved early second instar animals were supplemented with the indicated concentrations of [U-$^{13}C_3$]cysteine, [U-$^{13}C_6$]glucose or vehicle in the food during the indicated time. Sample were collected (5-6 biological replicates for labelled conditions, 4 biological replicates for unlabeled condition), and intracellular metabolites were extracted using 80% (v/v) aqueous methanol. Q1/Q3 SRM transitions for incorporation of 13C labeled metabolites were established for isotopomers for 65 polar metabolites and data were acquired by LC-MS/MS. Peak areas were generated using MultiQuant 2.1 software. The mean peak areas from unlabeled conditions were used for background determination and were subtracted from each corresponding 13C labelled dataset.

Immunostaining

Tissues from 68-85 hours AEL larvae were dissected in phosphate-buffered saline (PBS) 2% formaldehyde at room temperature, fixed 20-30 min in 4% formaldehyde, washed twice 10 min in PBS 0.3% Triton (PBST), blocked 30 min (PBST, 5% BSA, 2% FBS, 0.02% NaN3), incubated with primary antibodies in the blocking buffer overnight and washed 4 times for 15 min. Secondary antibodies diluted 1:200 or 1:500 in PBST were added for 1 hour and tissues washed 4 times before mounting in Vectashield/DAPI. Rabbit anti P-4EBP1 was from Cell Signaling Technologies (CST 236B4, #2855) and diluted 1:500, rabbit anti-tRFP was from Evrogen (#AB233) and used against mKate2 to stain cystinosin-mKate2. Samples were imaged using Zeiss LSM 780 and Leica TCS SP8 SMD confocal systems with a 40x water or 40x oil immersion objective and images were processed with Fiji software.

Western Blots

Tissues from 15-30 animals were dissected in CST lysis buffer (Cat#9803) containing 2x protease inhibitor (Roche, 04693159001) and 3x phosphatase inhibitor (Roche, 04906845001), and homogenized using 1 mm zirconium beads (Next Advance, ZROB10) in a Bullet Blender tissue homogenizer (Model BBX24, Next Advance). Protein content was measured to normalize samples, 2x Laemmli Sample Buffer (Biorad) was added and samples boiled 6 min @ 95°C. Lysates were resolved by electrophoresis (Mini-PROTEAN TGX Precast Gels, BioRad; or PAGEr EX Gels, Lonza; or home-made gels), proteins transferred onto PVDF membranes (Immobilon P, Millipore), blocked in Tris-buffered saline with or without 0.1% Tween-20 buffer containing 3 or 6% BSA, and probed with P-S6K antibody (1:1000, CST 9209). After P-S6K was revealed, membranes were stripped for 5-30 min (Restore PLUS Buffer, Thermo Scientific #46430), washed, blocked in PBS Tween-20 buffer containing 5% dry milk, and probed with S6K antibody (1:10000, a gift from Aurelio Teleman[25]). For normalization blots were probed with GADPH antibody (1:5000, GeneTex GTX100118). Data show representative results from at least 2 or 3 biological replicates. Horseradish peroxidase (HRP) conjugated secondary IgG antibodies (1:10000) were used together with the SuperSignal West Dura Extended Duration Substrate (Thermo Scientific #34076) to detect the protein bands.

Generation of clones

For autophagy experiments, clones were generated by crossing *yw,hs-Flp; mCherry–Atg8a; Act>CD2>GAL4, UAS–nlsGFP/TM6B* with the indicted UAS lines. Progeny of the relevant genotype was reared at 25°C and spontaneous clones were generated in the fat body due to the leakiness of the hs-flp. For *dCTNS*$^{-/-}$ clones, autophagy was analyzed by crossing *w;; neoFRT82B, dCTNS*$^{-/-}$ to *hsFlp; R4-Gal4, UAS-mCherry-Atg8a; FRT82B UAS-GFP/TM6b*. For P-4E-BP1 experiments, clones were either generated by crossing *hsFlp; act>CD2>Gal4, UAS nls GFP* with the indicted UAS lines or, for *dCTNS*$^{-/-}$ clones, by crossing *w;;neoFRT82B, dCTNS*$^{-/-}$ to *yw, hsFlp, Tub-Gal4>UAS-nlsGFP/FM6;;neoFRT82B, TubGal80/TM6,Tb,Hu*. F1 embryos collected overnight were heat shocked 3 times for 30 min.

Statistics

Experiments are presented with the mean +/- SEM. P values and significance: ^{ns}, $P \geq 0.05$; *, $P \leq 0.05$; **, $P \leq 0.01$; ***, $P \leq 0.005$; ****, $P \leq 0.0001$. **Life span experiments:** N=1 means average of 8-10 vials per genotype and condition in 1 experiment. Fig. 1j ($N \geq 5$), Fig. 3a (N=4), Fig. 4j (N=3-4): significance was determined by a two-tailed t-test (Mann-Whitney). **Pupariation assay:** Fig. 1k, Fig. 1l, Fig. 2d, Fig. 3a, Fig. 4j: significance was

determined by one-way ANOVA followed by a Bonferroni multiple comparisons test. **Cysteine measurements (Profoldin kit):** Fig. 1f, g: significance was determined by a one-way ANOVA followed by a Bonferroni multiple comparisons test. Fig. 1i: significance was determined by a two-tailed t-test (Mann-Whitney). **Western blots:** Fig 1h, Fig. 1i, Fig. 2e, Fig. 4i: significance was determined by one-way ANOVA followed by a Bonferroni multiple comparisons test. Fig 1a: spline curve represent the trend over multiple experiments. Fig 1b, 4a, 4b: significance was determined by two-way ANOVA followed by a Sidak's multiple comparisons test. Fig 2c, 2f, 4d: significance was determined by one-way ANOVA followed by a Tukey's multiple comparisons test. **Metabolomics:** Fig 2b, 2c: significance was determined by one-way ANOVA followed by a Tukey's multiple comparisons test. Fig 3d: significance was determined by a two-tailed t-test (Mann-Whitney).

SUPPLEMENTARY INFORMATION

SUPPLEMENTARY FIGURES & LEGENDS

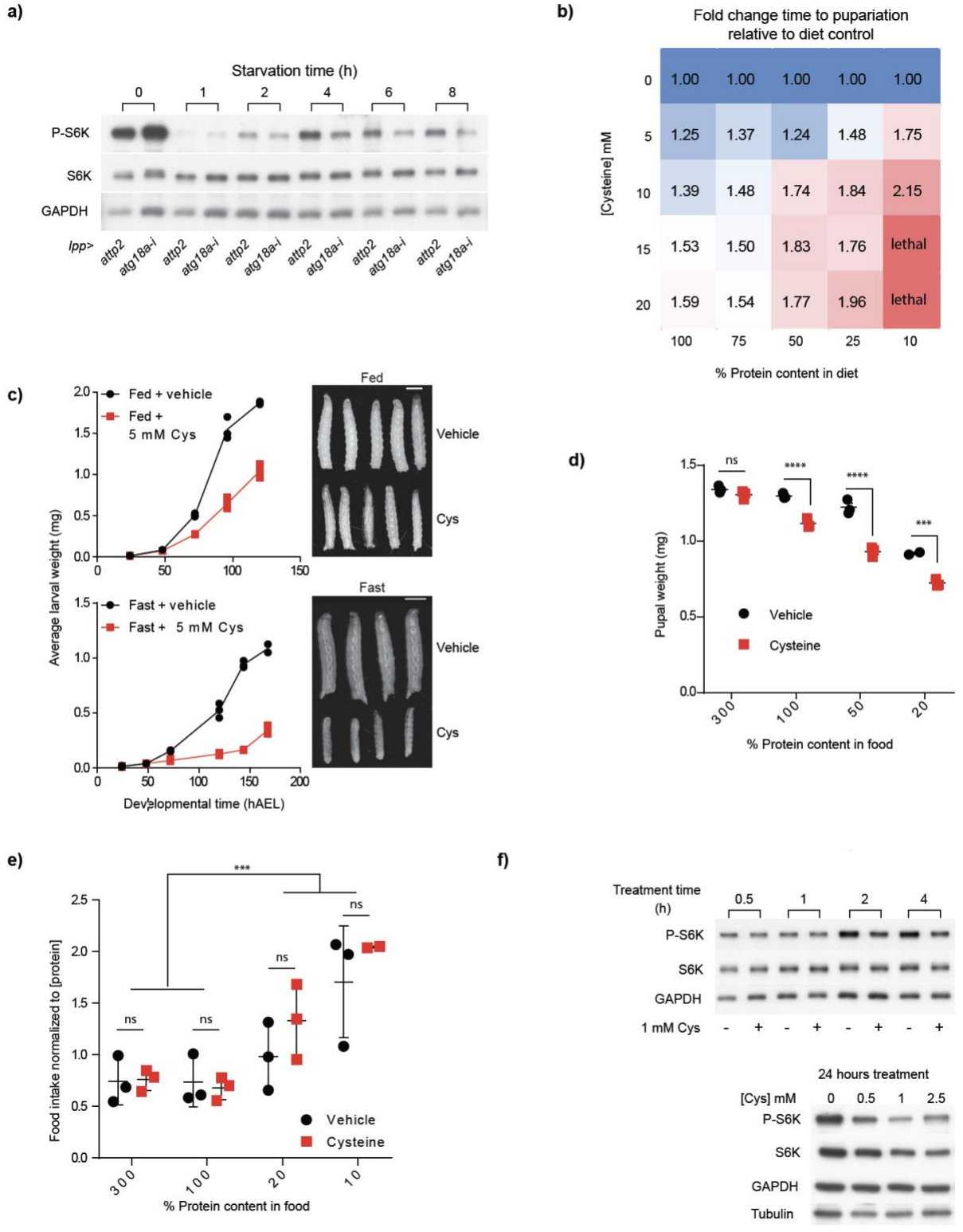

Extended Data Figure 1: Amino acid screen revealing cysteine as a growth suppressor. a) mTORC1 reactivation upon fasting requires autophagy. P-S6K levels +/- SEM in dissected fat body from control and fat body-expressing *Atg18a RNAi* larvae starved for the indicated time. b) Cysteine suppresses growth in a dose and diet dependent manner. Mean fold change time to pupariation (w^{1118} larvae) as a function of total protein content and cysteine concentration supplemented in the food. Data are normalized to control for each diet. c) Cysteine supplementation affects larval growth all along development. Growth curves (mean larval weight (mg)

+/- SEM as a function of time (hours AEL)) for *w1118* larvae fed ad libitum a 100% [AA] (top) or 10% [AA] (bottom) diet with 5 mM cysteine or vehicle. N=3. Pictures show age-matched larvae at 96 and 144 hours AEL in fed and fast conditions, respectively. Scale bar 1mm. d) Animals fed cysteine are reduced in adult size and this process is diet dependent. Pupal weight (mg) +/- SEM of w^{1118} larvae fed *ad libitum* 300, 100, 50 and 20% total protein diet with 10 mM cysteine or vehicle. Mean +/- SEM; ^{ns}, $P \geq 0.05$; ***, $P \leq 0.005$; ****$p \leq 0.0001$, multiple t-tests. e) Diet affects food intake whereas cysteine supplementation does not. Food intake normalized to protein content of larvae raised on the indicated diet with 5 mM cysteine or vehicle. ^{ns}, $P \geq 0.05$, two-tailed t-test.***$p \leq 0.005$; two-tailed t-test between all fed and starved conditions. f) Cysteine treatment inhibits mTORC1 activity. P-S6K levels in dissected fat body from larvae fed a full diet with the indicated concentrations of cysteine or vehicle for the indicated time. Prolonged cysteine treatment (bottom panel) cause downregulation of S6K levels.

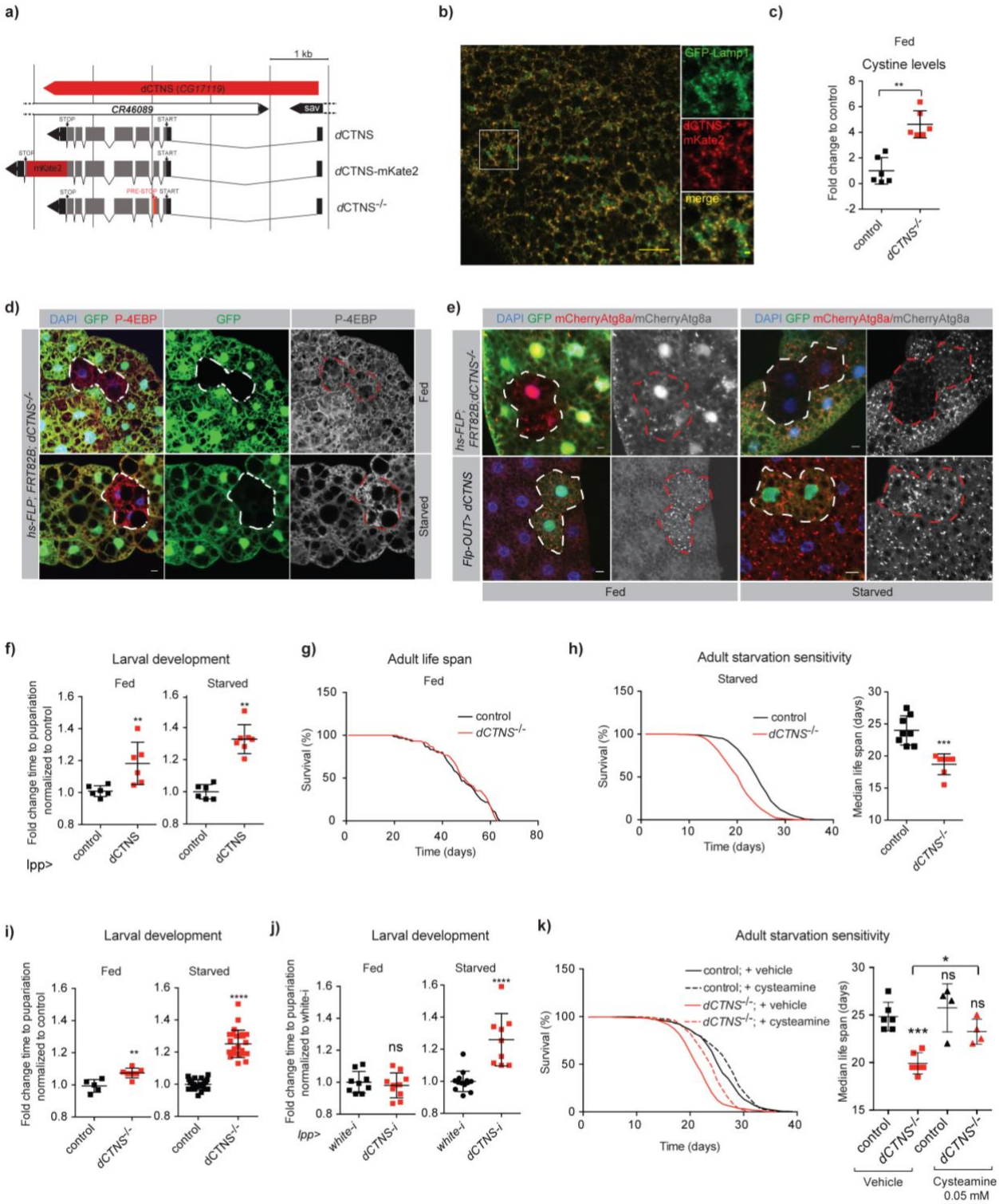

Extended Data Figure 2: Lysosomal cystine efflux controls resistance to starvation through autophagy. a) Schematic of the *dCTNS* locus and alleles generated by CRISPR/Cas9. *dCTNS-mKate2*, C-terminal insertion at the endogenous locus; *dCTNS*$^{-/-}$, frameshift mutant. b) Cystinosin is targeted to the lysosomal membrane. Co-localization of Cystinosin-mKate2 with the lysosomal membrane protein Lamp1-GFP in the fat body. Scale bar, 20 μm and 2 μm. c) *dCTNS*$^{-/-}$ larvae accumulate cystine. Cystine levels in whole third instar larvae lysates fed a standard diet. d) Cystinosin limits mTORC1 reactivation upon fasting. *dCTNS*$^{-/-}$ fat body clones (non-GFP, outlined) in 80hAEL animals starved for 24h and stained for P-4EBP. DAPI, blue; GFP, green; P-4EBP, red or white. Scale bar 10 μm. e) Cystinosin maintains autophagy during fasting. Fat body *dCTNS*$^{-/-}$ clones (upper panel, non-GFP, outlined) or flip-out clones overexpressing *dCTNS* (lower panel, GFP marked, outlined) in 80h AEL animals expressing mCherry-Atg8a starved for 8h. DAPI, blue; GFP, green; mCherry-Atg8a, red or white. Scale bar 10 μm. f) *dCTNS* overexpression in larval fat body causes

developmental delay. Fold change time to pupariation for larvae fed or fast *ad libitum*. g) Cystinosin does not affect lifespan in fed condition. Lifespan of control (w^{1118}) and $dCTNS^{-/-}$ animals fed standard food *ad libitum* condition. N=2. h) Cystinosin controls starvation resistance of adult animals. Lifespan of control (w^{1118}) and $dCTNS^{-/-}$ animals fed a chemically defined starvation medium *ad libitum*. i-j) Cystinosin in the fat body controls starvation resistance of larvae. Fold change time to pupariation of larvae of indicated genotype grown on fed or starved food. k) Cysteamine treatment restores starvation resistance of $dCTNS^{-/-}$ animals. Lifespan of control (w^{1118}) and $dCTNS^{-/-}$ animals fed *ad libitum* a chemically defined starvation medium supplemented with 0.5 mM cysteamine or vehicle. c, f, h-k) Mean +/- SEM; ^{ns}, $P \geq 0.05$; *, $P \leq 0.05$; **, $P \leq 0.01$; ***, $P \leq 0.005$; ****,$P \leq 0.0001$: significance was determined by a two-tailed t-test (Mann-Whitney). For life span, N=1 means average of 8-10 vials per genotype and condition in 1 experiment.

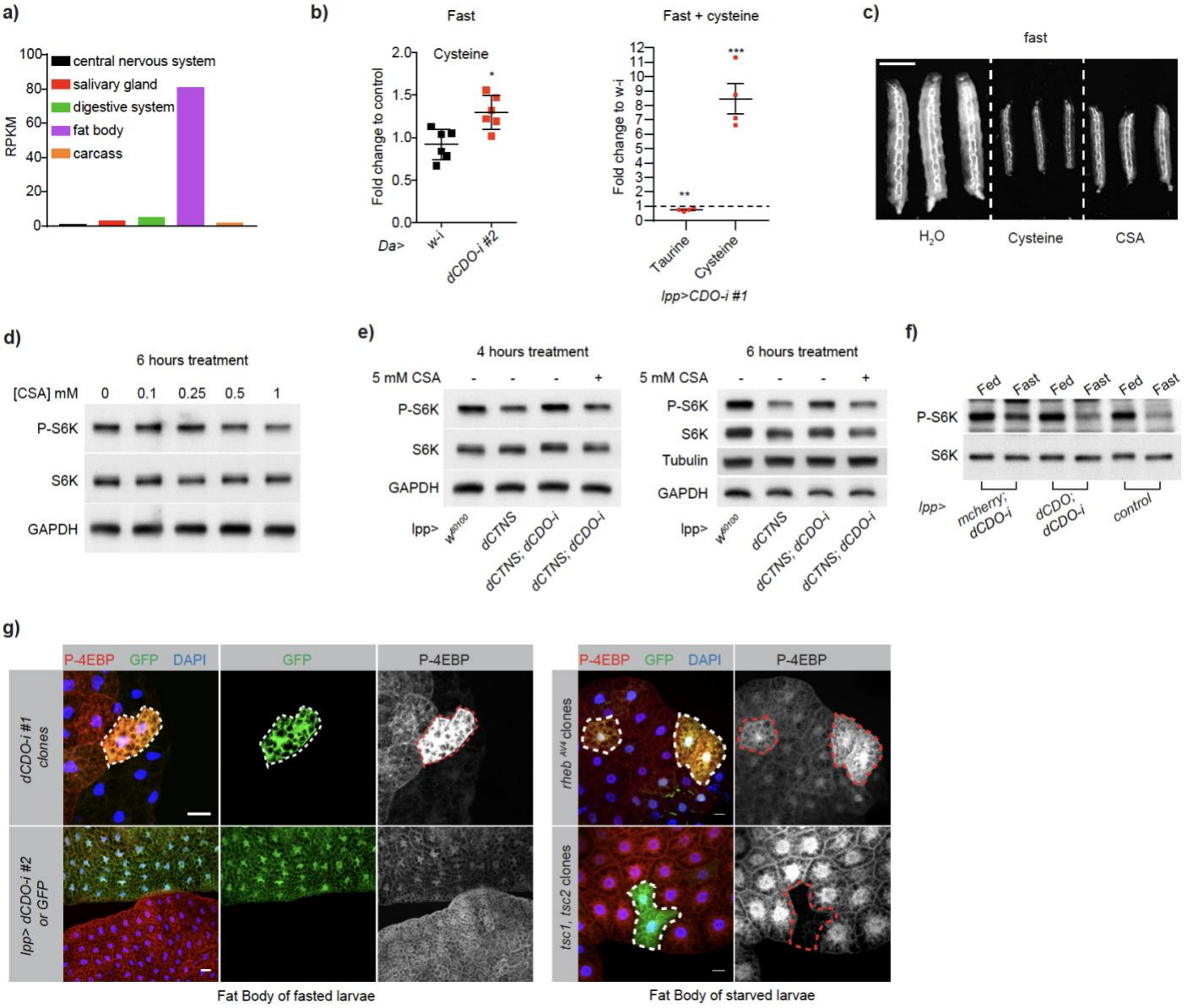

Extended Data Figure 3: Cysteine degradation by *dCDO* limits reactivation of mTORC1 under prolonged fasting. a) dCDO is enriched in the larval fat body. CG5493/dCDO expression (RPKM) in larval tissues from http://www.flyrnai.org/tools/dget/web. b) dCDO mediates cysteine degradation. Fold change concentrations of cysteine and taurine measured by Cysteine Assay Kit (left) and by LC-MS/MS (right) in whole third instar animals supplemented with 5 mM cysteine in a fasted diet for 24h (right), or without cysteine supplementation (left). Mean +/- SEM; *, P≤0.05; **, P≤0.01; ***, P≤0.005, two-tailed t-test. c-d) CSA (cysteine sulfinate) treatment phenocopies the effect of cysteine on growth and mTORC1 signaling. c) Age matched w^{1118} larvae (168h AEL) fasted *ad libitum* with 5 mM cysteine, 5 mM CSA or vehicle. Scale bar 1mm. d) P-S6K levels in dissected fat bodies from control larvae fed the indicated concentrations of CSA. e) CSA acts downstream cystinosin and dCDO to inhibit mTORC1 signaling. P-S6K levels in dissected fat bodies from larvae of indicated genotypes treated with vehicle or 5mM CSA for the indicated times. f) *CDO RNAi* fat body cells fail to limit S6K phosphorylation upon prolonged starvation, which is rescued by a *dCDO cDNA*. Western blot from dissected fat bodies of third instar animals of the indicated genotype (control is attp40), fed or fasted 12h. g) CDO is required to limit phosphorylation of the TORC1 target 4EBP upon prolonged fasting. Top panels: flip-out clones (marked by GFP, outlined) in the fat body expressing a *dCDO RNAi*. Bottom panel: fat body expressing either GFP or *dCDO RNAi*. Animals were fasted 24 hours and 80h AEL larvae were stained for P-4EBP. DAPI, blue; GFP green; P-4EBP red or white. Scale bar 20 μm.

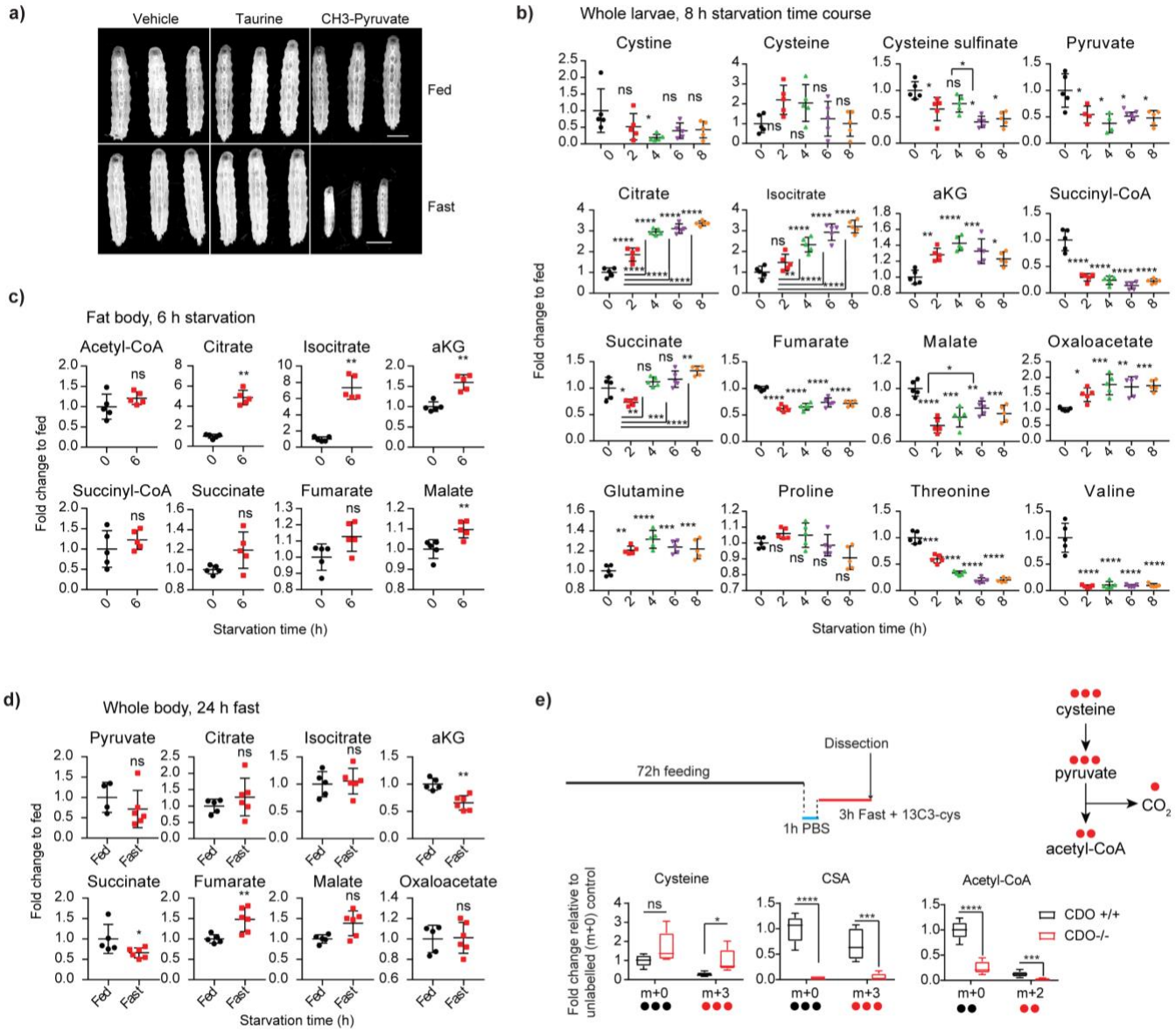

Extended Data Figure 4: Cysteine metabolism to acetyl-CoA maintains the level of TCA cycle intermediates upon fasting. a) Methyl-pyruvate but not taurine treatment phenocopies cysteine. Age matched *w*^{1118} larvae fed (120h AEL) and fasted (192h AEL) *ad libitum* with 5 mM cysteine, 5 mM methyl-pyruvate, 5 mM taurine or vehicle. Scale bar 1mm. b) Relative metabolite levels measured from whole mid-third instar larvae starved on PBS for the indicated time. c) Relative metabolite levels measured from dissected fat bodies of mid-third instar larvae fed or starved on PBS for 6h. d) Relative metabolite levels measured from whole mid-third instar larvae fasted 24h on a minimal diet. b-d) Mean +/- SD. e) Mean +/- SEM metabolite isotopologues abundance in dissected fat bodies from control and *CDO*$^{-/-}$ larvae supplemented with 5 mM $^{13}C_3$-cysteine for 3h in a fast diet. (N=5). b-e) ^{ns}, P≥0.05; *, P≤0.05; **, P≤0.01; ***, P≤0.005; ****p≤0.0001. One-way ANOVA followed by a Tukey's multiple comparisons test (b); two-tailed t-test (c-e).

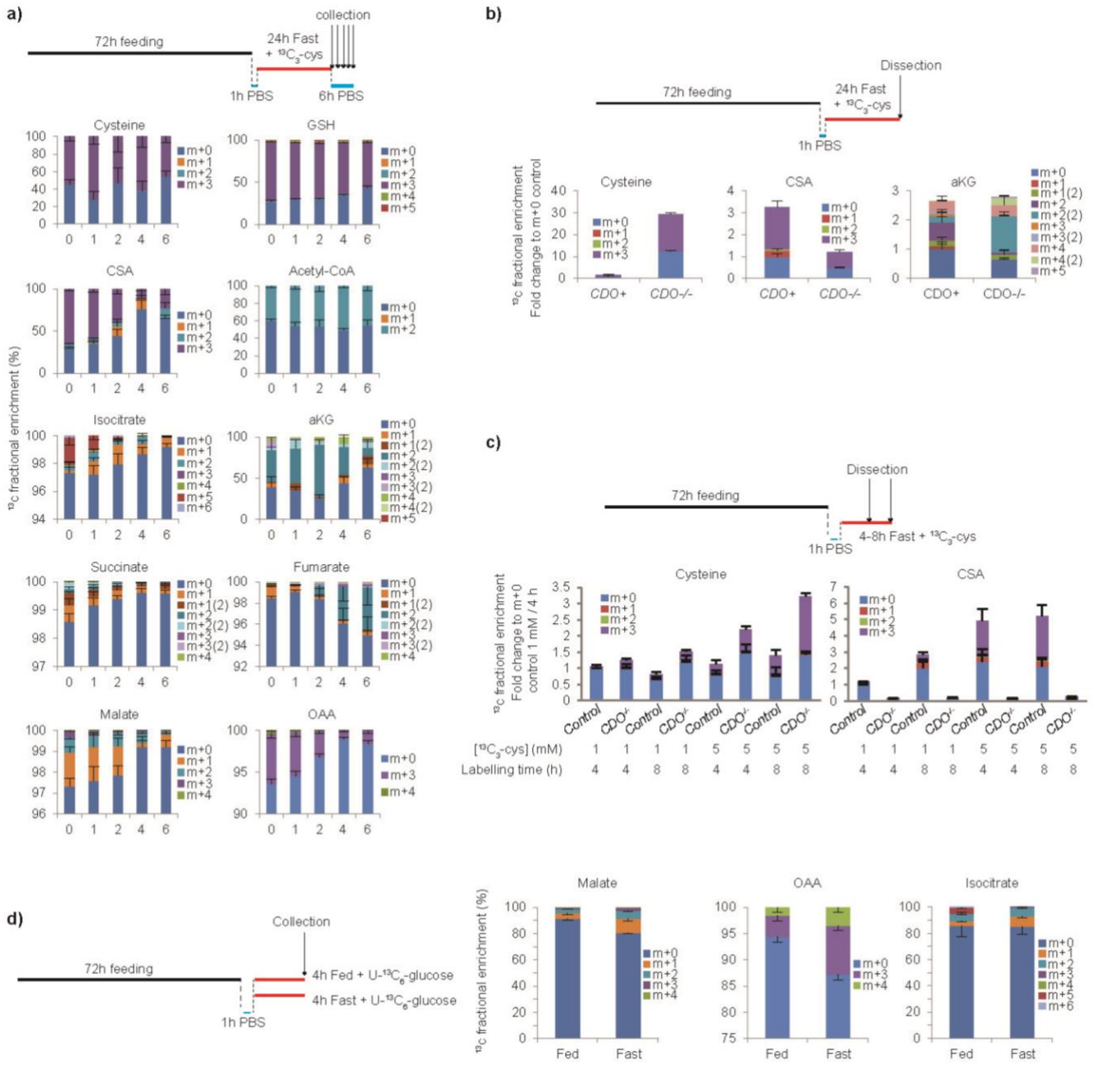

Extended Data Figure 5: TCA cycle intermediates labelling with $^{13}C_3$-cysteine. a-c) ^{13}C fractional enrichment (%) for metabolite isotopologues (different number of ^{13}C atoms) and isotopomers (^{13}C at different atomic position) measured in whole larvae (a,d) or dissected fat bodies (b,c). Starved animals were supplemented for the indicated time with 5 mM $^{13}C_3$-cysteine or 25 mM U-$^{13}C_6$-glucose or otherwise indicated in a fasted diet. For ^{13}C contribution in aKG and succinate, m+2 and m+3 isotopomers noted (2) depends on pathways other than direct entry of cysteine into the TCA cycle through PDHa and PC, respectively. GSH, glutathione; CSA, cysteine sulfinate; aKG, alpha-ketoglutarate; OAA, oxaloacetate.

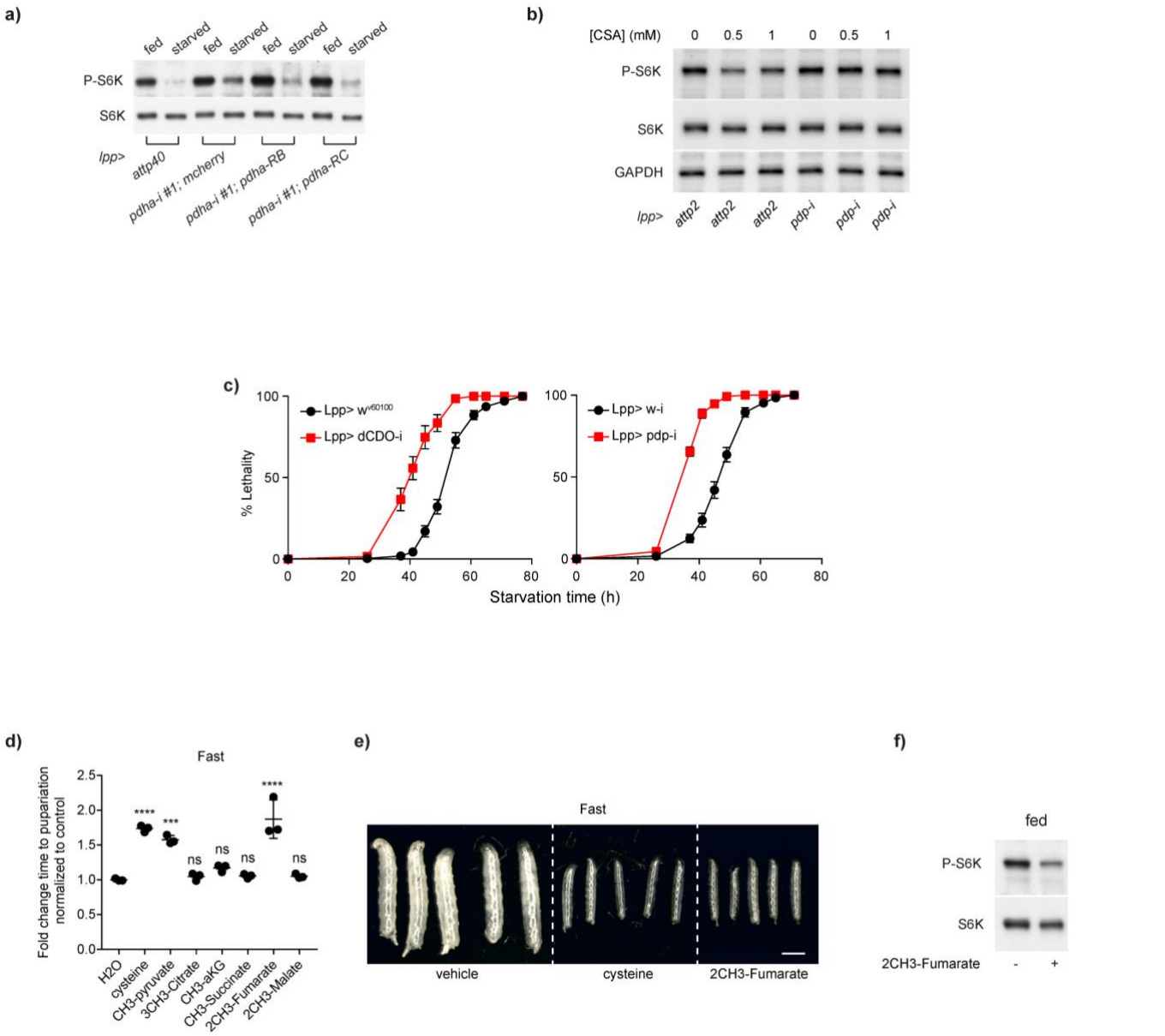

Extended Data Figure 6: The TCA cycle intermediate fumarate suppresses growth and mTORC1 signaling downstream CSA/acetyl-CoA. a) Knockdown of *pdha* in the fat body leads to higher reactivation of mTORC1 upon prolonged fasting, which is rescued by two isoforms of *pdha cDNA*. b) CSA suppresses mTORC1 through Pdp. P-S6K levels in fat body from fed larvae supplemented with CSA for 6h. c) Mean % lethality +/- SEM as a function of time (h) for 10 days old males of the indicated genotypes upon complete starvation (water/agar medium). N=10. d, e) A screen for growth suppression by TCA cycle intermediates reveals fumarate. d) Mean fold change time to pupariation for fasted w^{1118} larvae supplemented with the indicated metabolites in their methylated form or vehicle. ^{ns}, P≥0.05; ***, P≤0.005; ****p≤0.0001. One-way ANOVA followed by a Tukey's multiple comparisons test. e) Age matched fasted w^{1118} larvae supplemented with cysteine, dimethyl-fumarate or vehicle *ad libitum*. Scale bar, 1mm. f) P-S6K levels in dissected fat bodies from fed larvae supplemented with 10 mM dimethyl-fumarate or vehicle.

SUPPLEMENTARY TEXT

Supplementary Text 1: An amino acid supplementation screen reveals cysteine as a growth suppressor

To evaluate the effects of individual amino acids on growth, we developed an amino acid supplementation screen of developing *Drosophila* larvae and measured their development rate (Supplementary Methods). The screen identified cysteine as a strong growth suppressor (Fig. 1c), an effect that could be due to the cytotoxicity of cysteine previously reported in cell culture, yeast, and chicks[1-3]. However, we found that the effect of cysteine supplementation was diet dependent, with cysteine strongly suppressing growth upon starvation while having weaker effect in fed animals (Extended Data Fig. 1b-d), mitigating cytotoxicity as a unique explanation for this result. In addition, although the effect of cysteine on growth was dose dependent (Extended Data Fig. 1b), variation in cysteine intake between fed and starved conditions was not sufficient to explain the diet-dependent cytotoxicity (Extended Data Fig. 1e). Therefore, we conclude that the growth-suppressive effect of cysteine was multifactorial and decided to analyze the endogenous role of intracellular cysteine.

Supplementary Text 2: Developmental delay versus starvation sensitivity

Gain and loss of function of *dCTNS* have opposite effect on mTORC1 but showed similar phenotype in term of larval development: an increase in the time to pupariation. To avoid confusion between opposite processes that lead to similar phenotypes in appearance, we adapted our nomenclature accordingly. Because the loss of *dCTNS* caused reduced cellular cysteine, upregulation of mTOR, inhibition of autophagy, and that cysteine and rapamycin treatments rescued/accelerated the time to pupariation, we termed *CTNS*$^{-/-}$ developmental phenotypes “starvation sensitivity”. Accordingly, *CTNS*$^{-/-}$ did not affect development of fed larvae. By contrast, *dCTNS* overexpression increased cellular cysteine, downregulated mTORC1 and induced autophagy. In agreement with mTORC1 loss of function delaying larval growth and development, we termed the developmental phenotype of *dCTNS* overexpression “developmental delay”. Consistently, *dCTNS* overexpression retarded development in both fed and starved conditions.

Supplementary Text 3: $^{13}C_3$-cysteine labeling *in vivo*

We used $^{13}C_3$-cysteine supplementation in the food to follow cysteine carbons into the TCA cycle. We first fed animals 5 mM $^{13}C_3$-cysteine for 24 hours, and then analyzed labeling in the TCA cycle following different chasing times after placing animals on PBS. This allowed us to assess the dynamics and stability of labeling in order to further adjust our protocol for experiments on dissected fat bodies. Results showed variable but overall low incorporation of cysteine carbons in different TCA cycle intermediates, and the extent of labeling progressively reduced with chasing time for most metabolites (Extended Data Fig. 5a). This indicates that cysteine carbons enter the TCA cycle and that labeling is stable enough to allow for dissection time. However, labeling with 5 mM $^{13}C_3$-cysteine for 24 hours was not suitable to test the requirement of dCDO for cysteine entry in the TCA cycle in the fat body. Indeed, dissected fat bodies from *dCDO* mutant animals showed a >15-fold accumulation of labeled cysteine compared to control, thus mitigating conclusions regarding labeling in downstream metabolites in such different tracer concentrations (Extended Data Fig. 5b). To find a labeling protocol suitable to analyze the role of dCDO during cysteine entry in the TCA cycle, we analyzed $^{13}C_3$-cysteine concentration in control and *dCDO-/-* animals following shorter labeling time/lower tracer concentration (Extended Data Fig. 5c). Based on these experiments, we found that labeling with 5 mM $^{13}C_3$-cysteine for 3 hours was the best condition to avoid dramatic differences in tracer concentration in the fat body of control and *dCDO*$^{-/-}$ animals (Extended Data Fig. 4f, Extended Data Fig. 5c). Results showed that CDO mediates incorporation of cysteine carbons into CSA and Acetyl-CoA (Extended Data Fig. 4f). However, we could not conclude about pathway entry in the TCA cycle (PC vs PDHc) due to very low or absence of labeling in the TCA cycle using this protocol (data not shown). We further tried to force labeling in the TCA cycle intermediates in whole animals using 25 mM of [U-$^{13}C_6$]glucose for 4 hours. However, this also raised very limited labeling in TCA cycle (Extended Data Fig. 5d). Given these limitations, we decided to use genetics test the role of PC and PDHc in mediating the effect of cysteine on mTORC1.

SUPPLEMENTARY METHODS

Amino acid screen

We fed larvae a diet with reduced yeast extract/proteins (50% of normal diet), systematically added individual amino acids to the food (Table S1), and monitored the time to pupariation as a proxy for growth rate. The following mix was diluted 1:1 with amino acids solutions in water: 10g/L Agar; 120g/L Sucrose; 17g/L Deactivated Yeast extract; 83g/L Cornmeal; 6ml/L Propionic Acid; 20ml/L Tegosept. The amount of amino acids added to the food was determined based on those used in tissue culture growth supplements (Extended Data Table 1)[4-6].

	S2 medium [AA]mM	piper et al. [AA]mM	Lee et al. [AA]mM	Troen et al. [AA]mM	50x MEM [AA]mM	AA Screen [AA]mM
Glycine	3.3	25.6	5.7	13.3	5	10
L-Arginine hydrochloride	2.8	2.8	9.6	22.4	30	30
L-Aspartic acid	3.0	7.7	4.0	18.8	5	5
L-Cysteine hydrochloride	6.4	0.5	0.0	0.0		5
L-Cystine dihydrochloride	0.4	0.0	1.8	4.2	5	
L-Glutamic acid	5.4	10.2	8.2	38.1	5	5
L-Glutamine	12.3	10.3	8.2	0.0	5	5
L-Histidine hydrochloride	3.5	3.9	3.0	6.5	10	10
L-Isoleucine	1.1	13.9	6.2	14.5	20	20
L-Leucine	1.1	9.2	10.1	23.7	20	20
L-Lysine hydrochloride	11.3	7.8	19.0	44.5	20	20
L-Methionine	5.4	3.2	3.9	3 to 27	5	5
L-Phenylalanine	0.9	4.7	5.7	13.3	10	10
L-Proline	14.8	7.8	7.8	18.3	5	5
L-Serine	2.4	10.9	9.3	21.9	5	5
L-Threonine	2.9	10.1	7.6	17.6	20	5
L-Tryptophan	0.5	1.5	3.6	85.3	2.5	2.5
L-Tyrosine disodium salt	3.4	2.2	4.5	10.5	10	10
L-Valine	2.6	14.4	10.9	25.6	20	20
Alanine	0.0	23.6	12.5	29.2	5	5
Asparagine	0.0	7.7	4.0	0.0	5	5

Extended Data Table 1: Amino acid concentration used in the supplementation screen. Concentration of each amino acid (mM) used in Drosophila cell culture media (S2 medium), in three different published recipes for chemically defined food, in Minimum Essential Media (MEM) amino acid supplementation for cell culture, and in our amino acid add-back screen (Extended Data Fig. 1a).

Fly stocks

lpp-gal4 was a gift from Pierre Léopold; *UAS-tsc1, UAS-tsc2* a gift from Christen Mirth[7] ; *yw,hs-Flp; mCherry–Atg8a; Act>CD2>GAL4, UAS–nlsGFP/TM6B* a gift from Eric Baehrecke, *hsFlp; act>CD2>Gal4, UAS nls GFP* a stock from Norbert Perrimon lab[8], *yw, hsFlp, Tub-Gal4>UAS-nlsGFP/FM6;;neoFRT82B, TubGal80/TM6,Tb,Hu* a gift from Allison Bardin, *nprl2*^{1} a gift from M. Lilly and *hsFlp; R4-Gal4, UAS-mCherry-Atg8a; FRT82B UAS-GFP/TM6b* a gift from G. Juhász. The following stocks were obtained from BDSC: *UAS-w*^{RNAi} (HMS00045), *UAS-w*^{RNAi} (HMS00017), *attp40* (#36304), *attp2* (#36303), *UAS-mCherry-nls* (#38425), *UAS-PDHa*$^{RNAi\text{-}\#2}$ (HMC04032), *UAS-pdp*^{RNAi} (HMS01888), *UAS-CDO*$^{RNAi\text{-}\#1}$ (HMJ22159), *UAS-Atg1*^{RNAi} (HMS02750), *UAS-Atg18a*^{RNAi} (JF02898), *UAS-TSC2*^{RNAi} (HM04083), *w*^{1118}, *UAS-dCTNS*^{RNAi} (HMS00213). *w* (v60100), *UAS-CDO*$^{RNAi\text{-}\#2}$ (v50637) and *UAS-PDHa*$^{RNAi\text{-}\#1}$ (v40410) were obtained from VDRC. *UAS-PDHa-RB, UAS-PDHa-RC* and *UAS-CDO* were constructed using the FlyBi project Gateway ORFs collection (http://flybi.hms.harvard.edu/). The entry plasmids were used in a LR clonase reaction (Invitrogen, 11791-020), with the destination vector pWALIUM10-roe[9] or equivalent (Frederik Wirtz-Peitz, unpublished data). The plasmid was then microinjected into embryos which harbor attP2 or attp40 landing sites, as per standard procedures to create transgenic flies. When comparing the effects of RNAi knockdown, *UAS-w*^{RNAi} (HMS00045), *UAS-w*^{RNAi} (HMS00017), *attp2* (#36303) and *attp40* (#36304) were used as controls for the TRIP

collection (http://www.flyrnai.org/TRiP-HOME.html), and *w* (v60100) for the VDRC collection.

dCDO knockout flies were generated with the CRISPR/Cas9 technology according to [10]. Briefly, three sgRNA targeting the 5' end of the first exon and the last exon of *dCDO* (F/R sgRNA oligos sequences: GTCGCTCGGTGTCGATCTTGGACA/ AAACTGTCCAAGATCGACACCGAG; GTCGCAGCGGCTGATAGTAGCTAG/ AAACCTAGCTACTATCAGCCGCTG; GTCGAGGGTGGACAGTATAGGTGA/ AAACTCACCTATACTGTCCACCCT) were cloned in the pCFD3 expression vector. Plasmids were injected into *nos-Cas9* embryos and emerging adults crossed to *Sco/Cyo.* Progenies were screened by PCR for deletion of the whole *dCDO* locus and individual stocks were established, along with control lines that followed the same crosses scheme. Mutant stocks were sequence verified and further validated by qPCR. dCTNS knockout flies were generated with CRISPR/Cas9 technology according to[11]. Two sgRNA using oligos (one after the ATG start codon in exon 3: GGTGATGTCATGGGAATCGA, and the other before the translation of the first transmembrane domain in exon 4: GGGCAGTACTCGAAATCAGT) were produced by PCR and *in vitro* transcribed into RNA via MEGAscript™ T7 Transcription Kit (ThermoFisher). RNA was injected into ActCas9 flies (from Fillip Port/Simon Bullock). F0 flies were crossed to w;; TM3,Sb/TM6,Tb balancer flies and F1 progenies were screened via PCR by uisng oligos flanking the targeted genome region. Any indel difference > 3 bp was visualized in 4% agarose gel in heterozygot F1 progeny.

To generate *dCTNS-mKate2* fusion allele, *mKate2* open reading frame was inserted at the C-terminus of *dCTNS* through CRISPR/Cas9 endogenous tagging strategy using vectors kindly provided from Y. Bellaiche (Curie Institut, Paris). In brief, two 1 kb long homology arms (HR1, HR2) of the *dCTNS* gene flanking the sgRNA-guided Cas9 cutting site were cloned into a vector flanking the ATG/STOP-less *mKate2* allele (HR1-linker-mKate2-loxP-mini-white-loxP-linker-HR2). In addition, two vectors for the expression of sgRNA (sgRNA-1: CCACCGTGACCGATGTTCAAAAT, sgRNA-2: CCGAGCGAAGTGACGACTGAGAA) targeting the C-terminal coding region of *dCTNS* were generated. All three vectors were injected into vas-Cas9 flies (BDSC#55821) embryos by Bestgene. Progenies were screened for the red eyes (selection marker mini-white) and crossed to Cre-expressing flies to remove the mini-white by *loxP*/Cre excision. For overexpression of *dCTNS*, *dCTNS* cDNA was cloned into Gateway destination vector pUASg-HA.attB (GeneBank: KC896837) according to[12]. The plasmid was injected by Bestgene into FlyC31 embryos (BDSC#24482) for *ϕ31*-mediated recombination at a attP insertion site on the second chromosome.

Fly food and starvation protocols

All amino acids and compounds used were from Sigma. In N. Perrimon's lab compounds in solution were added to the following food mix: 60 g/L sucrose, the indicated amounts of deactivated yeast as a source of total protein (2 g/L for fast, 4 g/L for mildly fast, 20g/L for fed fly food); 80 g/L cornmeal, 0.35% Bacto Agar, 0.3% propionic acid, 1% tegosept (100g/L in ethanol). In the Simon's lab fasting food was adapted to 6 g/L of deactivated yeast to match control fast developmental rates observed in the Perrimon. For fed food, the standard lab food was used (see protocol above). In Extended Data Fig. 1 specifically, 100% amino-acid is 17g/L deactivated yeast.

Food intake

Larvae were synchronized in L1 and reared on the indicated food types until mid-2nd instar. Larvae were then transferred on the same food type supplemented with 0.5% weight/volume erioglaucine disodium salt (Sigma) for 2 hours. Samples were homogenized in 200 µl of PBS and absorbance of the dye in the supernatant was measured at 625 nm. Results were normalized to protein content.

Growth curves/pupal weight

Synchronized, newly-hatched L1 larvae were immediately weighed or placed on the indicated food at a density of 30-50 animals/vial. Pools of 20-80 animals were weighed every 24 hours using an analytical scale (Mettler Toledo) and the weight/animal was reported +/- SEM. For pupal weight, two-day-old pupae from vials at a density of 30 animals were weighed in batches of 5-10 pupae. The weights of different batches of larvae from the same vials were averaged and counted as N=1.

Starvation resistance assay

10-day-old adult males of the indicated genotypes reared on lab food at controlled density were transferred to

1% Bacto agar in water (20-25 animals/vials) and dead animals were scored every 4 or 6 hours starting at 24 hours of starvation.

Cysteine measurement

25-40 mid-second instar animals were homogenized in cold PBS 0.1% Triton and centrifuged at 4°C. Cysteine measurement was performed in triplicate from the supernatant using the MicroMolar Cysteine Assay Kit (ProFoldin, CYS200) according to the manufacturer's instructions. Data were normalized to protein content.

Cystine measurements

Larvae were washed three time (water, shortly in 70% ethanol, and in finally in PBS), dried on tissue paper and 10 larvae/sample were shock frozen in liquid nitrogen and stored at -80°C until lysis. Larvae were lysed in 80 µl of 5.2 mM N-ethylmaleimide, centrifuged 10 min at 4°C and 75 µl supernatant was deproteinized by addition of 25 µl of 12% sulfosalicylic acid. Protein-free supernatants were kept frozen at -80°C until analysis and centrifuged at 1,200 x g before use. Cystine quantification was performed using AccQ-Tag Ultra kit (Waters®) on a UPLC-xevoTQD system (Waters) according to the manufacturer's recommendations. Ten µL of samples were mixed with 10µL of a 30 µM internal standard solution (stable isotope of cystine), 70µL of borate buffer and 20µL of derivative solution and incubated at 55°C for at least 10 minutes. Derivatized samples were diluted with 150µL of ultrapurified water and 5 µL of the final mix were injected in the triple quadrupole mass spectrometer in positive mode. Transitions used for derivatized cystine quantification and the internal standard were respectively 291.2>171.1 and 294.2>171.1. Cystine values were normalized by protein content using the Lowry's method on protein pellets.

SUPPLEMENTARY REFERENCES

1 Dilger, R. N., Toue, S., Kimura, T., Sakai, R. & Baker, D. H. Excess dietary L-cysteine, but not L-cystine, is lethal for chicks but not for rats or pigs. *J. Nutr.* **137**, 331-338 (2007).

2 Kumar, A. *et al.* Homocysteine- and cysteine-mediated growth defect is not associated with induction of oxidative stress response genes in yeast. *Biochem. J.* **396**, 61-69, doi:10.1042/BJ20051411 (2006).

3 Nishiuch, Y., Sasaki, M., Nakayasu, M. & Oikawa, A. Cytotoxicity of cysteine in culture media. *In Vitro* **12**, 635-638 (1976).

4 Lee, W. C. & Micchelli, C. A. Development and characterization of a chemically defined food for Drosophila. *PLoS One* **8**, e67308, doi:10.1371/journal.pone.0067308 (2013).

5 Piper, M. D. *et al.* A holidic medium for Drosophila melanogaster. *Nat. Methods* **11**, 100-105, doi:10.1038/nmeth.2731 (2014).

6 Troen, A. M. *et al.* Lifespan modification by glucose and methionine in Drosophila melanogaster fed a chemically defined diet. *Age (Dordr)* **29**, 29-39, doi:10.1007/s11357-006-9018-4 (2007).

7 Koyama, T. & Mirth, C. K. Growth-Blocking Peptides As Nutrition-Sensitive Signals for Insulin Secretion and Body Size Regulation. *PLoS Biol.* **14**, e1002392, doi:10.1371/journal.pbio.1002392 (2016).

8 Karpowicz, P., Zhang, Y., Hogenesch, J. B., Emery, P. & Perrimon, N. The circadian clock gates the intestinal stem cell regenerative state. *Cell Rep* **3**, 996-1004, doi:10.1016/j.celrep.2013.03.016 (2013).

9 Ni, J. Q. *et al.* Vector and parameters for targeted transgenic RNA interference in Drosophila melanogaster. *Nat. Methods* **5**, 49-51, doi:10.1038/nmeth1146 (2008).

10 Housden, B. E., Lin, S. & Perrimon, N. Cas9-based genome editing in Drosophila. *Methods Enzymol.* **546**, 415-439, doi:10.1016/b978-0-12-801185-0.00019-2 (2014).

11 Bassett, Andrew R., Tibbit, C., Ponting, Chris P. & Liu, J.-L. Highly Efficient Targeted Mutagenesis of Drosophila with the CRISPR/Cas9 System. *Cell Reports* **6**, 1178-1179, doi:https://doi.org/10.1016/j.celrep.2014.03.017 (2014).

12 Bischof, J. *et al.* A versatile platform for creating a comprehensive UAS-ORFeome library in Drosophila. *Development* **140**, 2434-2442, doi:10.1242/dev.088757 (2013).